For P

Low Compression Ratio Diesel Engines fuelled with Biodiesel by using Spark-Induced Compression Ignition(SICI)

Journal:	*International Journal of Engine Research*
Manuscript ID:	IJER-14-0027.R2
Manuscript Type:	Standard Article
Date Submitted by the Author:	n/a
Complete List of Authors:	Yamane, Koji; The University of Shiga Prefecture, Department of Mechanical Systems Engineering Kondo, Chihiro; The University of Shiga Prefecture, Department of Mechanical Systems Engineering Kondo, Daichi; Graduate School of Engineering, The University of Shiga Prefecture, Mechanical Systems Engineering Kawasaki, Kiyoshi; The University of Shiga Prefecture, Department of Mechanical Systems Engineering
Keywords:	Biodiesel, Low Compression Ratio, Diesel Engines, Combustion, Spark
Abstract:	The objective of this study is to demonstrate a novel combustion system in which auto-ignition is induced by spark discharge into a pre-mixture formed during a long ignition delay time at a direct injection(DI) diesel engine with a low compression ratio. An experiment is conducted to investigate the potential of spark discharge on the auto-ignition process by changing the spark timing, injection timing, equivalence ratio, and fuel amount. The fuel used is lauric methyl ester, which is a fatty acid methyl ester that has relatively higher volatility and higher ignition quality than petro diesel fuel. The results obtained by single cylinder common-rail DI diesel engine show that with a volumetric efficiency of 34%, spark-induced compression ignition (SICI) combustion is observed. In this study, the auto-ignition timing is advanced by spark discharge and is controlled by the spark timing within 5 deg. CA. We also observed SICI combustion flame by constant volume combustion vessel using direct flame high-speed photography and OH radical chemiluminescence spectroscopy by means of the combination of an optical band-pass filter, an image intensifier and CCD camera. As a result, it was found that SICI occurs not by flame propagation due to spark ignition but by auto-ignition of pre-mixture

	formed by spray. It was also clear that the auto-ignition is induced by transportation of OH radical at spark plug with spray flow.

SCHOLARONE™
Manuscripts

For Peer Review

Low Compression Ratio Diesel Engines

Fuelled with Biodiesel by using Spark-Induced Compression Ignition (SICI)

Koji Yamane, Chihiro Kondo, Daichi Kondo and Kiyoshi Kawasaki

Dept. of Mechanical Systems Engineering, The University of Shiga Prefecture, Japan

(yamane@mech.usp.ac.jp)

For Peer Review

ABSTRACT

The objective of this study was to demonstrate a novel combustion system in which autoignition is induced by spark discharge into a pre-mixture formed during a long ignition delay time in a direct injection (DI) diesel engine with a low compression ratio. The effects of spark discharge on the autoignition process were investigated by changing the spark timing, injection timing, equivalence ratio and fuel amount. The fuel used was lauric acid methyl ester, a fatty acid methyl ester that is relatively volatile and exhibits higher ignition quality than standard diesel fuel. The results obtained with a single cylinder common-rail DI diesel engine show that spark-induced compression ignition (SICI) combustion was obtained with a volumetric efficiency of 34%. In this study, the autoignition timing was advanced by spark discharge and was controlled by the spark timing within 5° CA. We also observed the SICI combustion flame in a constant volume combustion vessel using direct high-speed photography and OH radical chemiluminescence spectroscopy by means of a combination of an optical band-pass filter, an image intensifier and a CCD camera. The results showed that SICI occurs not by flame propagation due to spark ignition but by autoignition of a spray pre-mixture. It was also evident that autoignition is induced by transportation of OH radicals formed at the spark plug by the spray flow.

Keywords : Biodiesel, Low Compression Ratio, Diesel Engines, Combustion, Spark

For Peer Review

1. INTRODUCTION

It is well known that a low compression ratio (LCR) is desirable in diesel engines [1,2]. According to Miyamoto et al. [3], and as shown in Fig. 1, the change induced in the cooling loss (ψ_w) by reduction of the compression ratio from 16:1 to 12:1 is about 5%, whereas the change associated with reducing the ratio from 16:1 to 13:1 is minimal. In contrast, the degree of constant volume (η_{glh}) consistently increases as the compression ratio is decreased. For this reason, the rate of decrease of thermal efficiency with decreases in the compression ratio as determined by considering ψ_w and η_{glh} is lower than the rate of decrease of the theoretical thermal efficiency (η_{th}), as shown in Fig. 2. In addition, the application of a LCR is associated with low maximum pressure in the cylinder. The result is that both mechanical loss and heat loss are reduced, such that the brake thermal efficiency of a LCR engine can equal that of a high compression ratio engine.

In terms of exhaust emissions, a LCR leads to longer ignition delay times, allowing sufficient time for the formation of a lean mixture and so reducing the quantities of NOx and soot produced. However, this long ignition delay time also makes starting difficult under cold conditions, inducing unstable combustion under low loads and making active control of the ignition timing challenging.

The present study investigated the application of spark discharge in LCR diesel engines to overcome these problems. This approach involves the application of autoignition, induced by spark discharge, of a pre-mixture formed during the long ignition delay time resulting from the LCR. Spark-assisted diesel engines have been investigated by several researchers, and one prior publication has noted problems with plug fouling in spark-ignited diesel engines with a compression ratio of 12.1:1 [4]. Dhinagar et al. [5] reported that a low heat rejection, spark-assisted diesel engine fueled with diesel and operating at a compression ratio of 12.5:1 gave the best performance among the tested configurations, with an improved thermal efficiency of 3% and a reduced exhaust smoke level of 1.5 Bosch

For Peer Review

units, compared with a standard diesel engine operating at a compression ratio of 16.5:1. Fritz and Abata [6] investigated the cold start characteristics of a spark-assisted diesel engine operating on broad cut diesel fuel. Phatak and Komiyama [7] also reported that optimal performance was obtained at a compression ratio of 12.2:1 and a swirl ratio of 10 in a spark-assisted engine fuelled with DF-2 along with 20% methanol emulsified fuel. Persson et al. [8] found that the spark-assisted compression ignition (SACI) mode in a compression ignition engine with a compression ratio of 9.1:1, running on an ethanol/n-heptane fuel blend, was achieved by operating with a negative valve overlap (NVO) and trapping hot residuals. The SACI mode in that study was defined as combustion on the borderline between spark ignition (SI) and homogeneous charge compression ignition (HCCI) combustion modes.

The effects of spark discharge on ignition and on the combustion process, especially when employing a fuel with a high cetane number, have been investigated by several researchers. Examples include Ando et al. [9], Kuwahara et al. [10] and Nagamine et al. [11], who demonstrated these effects using a simulation of the chemical reaction process, employing a rapid compression machine (RCM) and dimethyl ether (DME) as the fuel. However, there has been little research concerning the control of ignition and

For Peer Review

combustion in LCR direct injection diesel engines by spark discharge into a pre-mixture formed by a high cetane number fuel.

This paper reports an experimental study investigating the effects of spark discharge on the autoignition process while varying the spark timings, injection timings, equivalence ratios and fuel amounts.

Additionally, we observed the SICI combustion flame in a constant volume combustion vessel using direct flame photography and OH radicals chemiluminescent spectroscopy, by means of a combination of optical band-pass filters. During these studies, lauric acid methyl ester (LaME) was used as a high cetane number fuel. LaME is a fatty acid methyl ester (FAME) that exhibits high volatility and good ignition quality. This material also represents a biodiesel fuel derived from plant oil and thus its use does not contribute to the global carbon dioxide burden.

For Peer Review

2. SICI COMBUSTION CONCEPT

Spark induced compression ignition (SICI) combustion involves autoignition induced by spark discharge and represents a new process that makes it possible to realize stable combustion by combining a low compression diesel engine and spark discharge along with a FAME that has high ignitability and high volatility. As shown in Fig. 3, this process involves several steps. Initially, a low compression ratio is applied to lean out the pre-mixture and to increase the ignition delay time, thus generating unstable combustion. Secondly, during the elongated ignition delay time, autoignition is induced by spark discharge into a lean pre-mixture to achieve stable combustion, active control of ignition timing and improved starting performance. Finally, as a result of employing a FAME with a high cetane number and high volatility as the fuel, the probability of inducing ignition is increased.

This SICI combustion concept, incorporating LCR, represents a promising means of reducing exhaust emissions and achieving high combustion efficiency through decreased friction. The practical applications of this concept will also contribute to an overall reduction in carbon dioxide emissions as a result of the use of biodiesel fuels based on FAMEs.

For Peer Review

3. EXPERIMENTAL APPROACH

3.1 Fuel Properties

Engine tests were carried out using LaME as the fuel (Paster M-12, Lion Co., Japan). In contrast to typical FAMEs made from rapeseed or soybean oils, LaME is a methyl ester derived from a short chain fatty acid that accounts for approximately 50% of the fatty acid content of coconut oil. The characteristic properties of LaME are provided in Table 1, which also shows the characteristics of gas oil as a comparison. In a previous paper [12], it was shown that LaME exhibits both a relatively low boiling point compared to typical FAMEs and high ignition quality. The cetane number (CN_{CFR} as measured in a CFR engine) of this fuel is also provided in Table 1 and demonstrates that LaME has almost the same ignitability as gas oil.

3.2 Engine Tests

Fig. 4 shows a schematic illustration of the experimental setup, while Table 2 presents the main specifications of the test engine. A single-cylinder water-cooled direct injection (DI) diesel engine (FD-1, Nissan Diesel Co., Japan) with a common-rail system (ECD-U2, Denso Co., Japan) was used during all experimental trials. The combustion chamber employed incorporated a shallow dish-type design in which the ratio of the diameter of the chamber, d, to the diameter of the bore, D, was $d/D = 0.86$, and in which the chamber depth was $H = 7.0$ mm [13]. The compression ratio was fixed at 14:1 during the trials. A butterfly valve was installed in the intake manifold to control the intake airflow rate. The swirl number was about 0.7 under wide open throttle (WOT) conditions and a

For Peer Review

spark plug (VFKH16, Denso Co., Japan) and ignition coil intended for use in passenger vehicles (FK0356, Diamond Electric Co., Japan) were used. The discharge energy was fixed at 30 mJ and the discharge time was held constant at 1.2 ms.

Fig. 5 presents a schematic showing the positions of the spark plug and injection nozzle. The spark plug was positioned such that the tip of the negative electrode was located inside the skirt of the combustion chamber and was vertically 3 mm from the cylinder head. As a result, one of the five fuel sprays was always close to the electrode.

During the experimental trials, the engine speed, injection pressure and coolant temperature were maintained at 1800 rpm, 100 MPa and 80 °C, respectively. The cylinder pressure and the nozzle needle lift were measured using a piezoelectric transducer (6053CCsp, Kistler Japan Co., Ltd.) and a hall-effect transducer, respectively. The signals from all of the above instruments were input into an engine combustion analyzer (DL-750, Yokogawa Electric Co., Japan) to calculate the rate of heat release. The spark signal was generated by a timing controller (LC220, Lab Smith Co., U.S.A.), using a crankshaft and the TDC signals.

3.3 Visualization of Ignition and Combustion

Figs. 6(a) and 6(b) show the experimental setup employed for visualization of

For Peer Review

ignition and combustion in the constant volume combustion vessel. The combustion vessel had a volume of 700 cc and its inner wall was heated electrically. The designated quantity of high-pressure fuel was pumped into the chamber by a manually operated high-pressure pump and the fuel was injected by a common-rail injector (number of holes = 7, nozzle orifice diameter = 0.157 mm, DENSO Co.). Although the nozzle orifice diameter of the constant volume combustion vessel differed from the 0.18-mm diameter used in the LCR engine, momentum theory predicts that both instruments will exhibit similar development of the fuel spray in the vicinity of the spark plug. In addition, the swirl airflow has little effect on the engine combustion characteristics when the spark plug and spray are situated in their present locations, since the swirl intensity in the experimental LCR engine is quite weak due to the low swirl number of 0.7 and the use of a very shallow, flat bottomed dish-type combustion chamber.

The same spark plug and pressure transducer as had been employed in the test engine setup were installed in this apparatus. The times at which injection and combustion events occurred were recorded using a high-speed video camera facing a quartz glass window. An optical interference band-pass filter and a CCD camera with an image-intensifier were also used to detect the chemiluminescence of OH radicals generated during autoignition and combustion. The central wavelength of the optical interference band-pass

For Peer Review

filter was 314.5 nm and its full width at half maximum (FWHM) was between 309 and 320 nm.

In this study, high-temperature, high-pressure conditions were created to simulate diesel combustion through the spark-ignited combustion of a hydrogen/oxygen/nitrogen gas pre-mixture. The spark plug was also used to trigger SICI combustion. Fig. 7 shows the procedure applied when simulating diesel-like conditions, based on changes over time in the pressure of the constant volume combustion vessel. The vessel is initially filled to a pre-determined density with a premixed hydrogen/oxygen/nitrogen combination. This mixture is then ignited by a spark electrode, creating a high-temperature, high-pressure environment through combustion of the initial premix. The gases in the vessel subsequently cool due to heat transfer to the vessel walls and the pressure slowly decreases.

During this pressure decay, the diesel fuel injector is actuated when the desired pressure is reached. When the pressure in the vessel reaches 1.5 MPa, fuel injection is initiated using the common-rail injector at a rail pressure of 40 MPa. The gas temperature in the vessel was maintained at approximately 790 K in each experimental trial by the precombustion of the gas mixture and by insulation of the vessel walls. The gas temperature was estimated by equilibrium calculation based on gas composition and gas pressure in the vessel. If suitable conditions exist at this point, autoignition and combustion of the diesel

For Peer Review

spray occur and the second pressure rise shown in this figure is generated. In the present study, SICI combustion was executed in this manner via discharge of the spark electrode.

4. RESULTS AND DISCUSSION

4.1 Effects of Spark Discharge on Autoignition

Typically, a two-stage heat release process is observed during diesel combustion with a long ignition delay. Combustion in the first stage is controlled by low temperature reactions (LTRs), while second-stage combustion (the rapid combustion phase) is associated with high-temperature reactions (HTRs). As a means of investigating the effects of spark discharge on heat release in the first stage and to determine whether or not this discharge induces a second heat release, a spark was discharged around the crank angle at the onset of the first heat release. In the experimental trials, the effects of spark discharge on autoignition were investigated under conditions in which the fuel quantity, Q, was equal to 1.1 kJ/cycle, which is equivalent to a low load at which the brake mean effective pressure is 0.2 MPa. Using a butterfly valve, the volumetric efficiency, η_v, was maintained at 34 vol% (an equivalence ratio of ϕ = 0.93). These experimental conditions were selected

For Peer Review

so as to attain SICI combustion at a low engine load approximating those associated with engine restart.

Fig. 8 shows the experimental results obtained in trials employing three spark timing and without spark discharge. When employing 19° BTDC spark timing, the heat release plot is composed of two distinct patterns and the ignition timing of the second heat release over several cycles is advanced by about 5° CA. When the spark timing, θ_{sp}, is set to coincide with the maximum of the first heat release rate (θ_p =11° BTDC), the ignition timing of the second heat release in all cycles is advanced by about 5° CA. It therefore appears that there is a relationship between the liquid spray after fuel injection end and the energy discharge timing of the spark plug.

4.2 Effects of Spark Discharge Timing

Fig. 9 shows the effects of spark discharge timing on the ignition timing and the heat release rate. When applying earlier spark timing, the heat output between the first release and second significant heat releases is enhanced, and thus the ignition timing of the second heat release occurs sooner. This occurs because the radicals supplied by the spark discharge induce local heat release. The highest intensity of radicals is generated by a stoichiometric combustion mixture. For this reason, we believe that a stoichiometric spray

For Peer Review

mixture exists in the vicinity of the spark gap and that the spark energy initiates the chemical oxidation reaction of the mixture, which in turn generates chemical species such as OH radicals. With earlier spark timing, the distribution of the pre-mixture around the spark plug is suitable for flame propagation and thus the heat release rate increases between the end of the first heat release and the start of the second heat release.

4.3 Effects of Equivalence Ratio

Fig. 10 summarizes the effects of the equivalence ratio on SICI combustion. Here, the equivalence ratio was changed from $\phi = 0.93$ to $\phi = 0.76$. This figure demonstrates that the timing of the SICI combustion was essentially unchanged between these two conditions, despite the change in the equivalence ratio. Therefore SICI combustion is able to control the ignition timing and achieve stable combustion even when the amount of fuel is varied.

4.4 Conditions Necessary to Achieve SICI Combustion

To clarify the conditions affecting SICI combustion, the injection timing and ignition timing were both varied, while maintaining the amount of fuel supplied such that Q = 1.1 kJ/cycle, and applying a volumetric efficiency of $\eta_v = 34$ vol%. Herein, combustion during which the change in ignition timing is less than 1° CA, even with spark discharge, is

For Peer Review

defined as conventional compression ignition (CI) combustion, while combustion in which the heat release gradually increases, such as in the case of flame propagation triggered by spark discharge, is defined as SI combustion.

Fig. 11 shows the combustion modes associated with various combinations of $\Delta\theta$, (the difference between spark timing (θ_{sp}) and injection timing (θ_j)) and θ_j. In these experiment trials, θ_j was varied when the ignition timing was nearly at top dead center (TDC) and when a misfire was observed on the after top dead center (ATDC) side.

In Fig. 11, SICI combustion is observed over a very narrow range of $\Delta\theta$ values (from 8 to 18° CA) at any value of θ_j (from -26 to -18° ATDC), as indicated by the unfilled circle symbols. Over the range of θ_j values, as $\Delta\theta$ is increased beyond 20° CA, the effects of spark discharge on autoignition are not observed and conventional CI combustion occurs, as indicated by the cross symbols. At equivalent θ_j values, as $\Delta\theta$ becomes less than 5° CA, the heat release rate diagram is divided into two patterns, as shown by the triangle symbols. At θ_j values greater than -18° ATDC, misfiring is observed without spark discharge and a gradual increase in heat release is observed with spark discharge, as indicated by the square symbols.

The conditions affecting SICI combustion may be discussed based on the relationship between the heat release rate diagram and the spark timing presented in Fig. 8.

For Peer Review

SICI combustion is not observed when $\Delta\theta$ is less than 5° CA since the pre-mixture does not reach the area near the spark plug, or because the pre-mixture has significant momentum due to the initial spray motion during the enlargement of the primary flame kernel. For this reason, when θ_{sp} equals 19° BTDC ($\Delta\theta$ = 5° CA), the heat release rate diagram is divided into two patterns, as can be seen in Fig. 8.

SICI combustion is not observed when $\Delta\theta$ is greater than 18° CA, presumably because autoignition over the entire combustion area occurs prior to the local heat release induced by spark discharge is adequate, due to the insufficient rate of chemical reaction or a delay in the enlargement of the initial flame kernel caused by a decreased quantity of pre-mixture near the spark plug. Therefore, this limit can possibly be extended by several means: adjusting the position of the spark plug, forming an adequate pre-mixture near the spark plug or increasing the discharge energy. The difference between the spark timing and the ignition timing advanced by spark discharge is about 5° CA and so, to achieve SICI combustion under these conditions, it may be necessary to increase the delay time beyond 5° CA between the onset times of the first and second heat releases. However, this delay is likely related to the properties of the pre-mixture near the spark plug and the flow motion, the details of which will be studied in future investigations employing a constant volume vessel and an optical path.

For Peer Review

When θ_j is later than -15° ATDC (between the square and triangle symbols), autoignition does not occur - even with the small amount of heat release induced by the spark discharge – due to the significant drop in temperature resulting from the falling motion of the piston.

The results shown in Fig. 11 may only apply at the compression ratio of 14:1 employed in the present study. In the case of higher compression ratios, the gas temperature at the end of the compression stroke is higher. For this reason, conventional CI combustion will occur under all conditions and the effects of spark discharge on autoignition will not be observed. When lower compression ratios are applied, however, conventional CI combustion will not take place due to the lower compression-end gas temperature.

For Peer Review

4.5 Effects of SICI Combustion on Starting in LCR Engines

It is possible to improve starting performance in low compression diesel engines under SICI combustion. Fig. 12 shows the temporal variations in the cylinder pressure, heat release rate and needle lift at a θ_j value of 18° BTDC.

When the engine is started without spark discharge, the resulting combustion is unstable and misfires occur. In addition, the ignition timing is extremely retarded, as shown in Fig. 12(a). To obtain regular ignition and stable combustion, the spark was discharged at

5° BTDC, after which the ignition timing was advanced and SICI combustion with a low COV took place, as in Fig. 12(b). Furthermore, after several SICI combustion cycles, when sparking once more ceased, stable autoignition was observed at the usual diesel combustion timing with a low COV, as shown in Fig. 12(c). This occurs because the temperature of the vessel walls rise to a steady state condition due to the previous stable SICI combustion cycles. As a result, SICI results in a stable value of indicated mean effective pressure (IMEP) following several unstable cycles, as shown in Fig. 13.

These results indicate that SICI combustion can warm up an engine and improve starting performance when a LCR is used. Even though the temperature of the engine and the intake air taken from a cold atmosphere will be relatively low compared with our experimental conditions, such that the temperature at the end of the compression stroke approaches low volumetric efficiency and the flow motion in the cylinder is reduced due to the low engine speed, these conditions increase the likelihood of SICI combustion in a cold atmosphere.

4.6 Direct Flame and OH Radical Imaging during SICI Combustion in a Constant Volume Combustion Vessel

For Peer Review

Figs. 14 and 15 present the time history of OH radical images and direct flame images during ignition and combustion processes, along with the rate of heat release. In the case of ordinary spray autoignition and combustion without spark discharge, luminescence from OH radicals is observed at approximately 3 ms, as seen in Fig. 14. In contrast, Fig. 15 shows that the application of spark discharge causes luminescence from OH radicals to appear sooner.

Based on the result obtained from visualization of ignition and combustion, several statements may be made concerning the ignition mechanism associated with SICI. As shown in Fig. 16, the ignition kernel, including OH radicals, is initially generated by the spark discharge. This kernel is transported by the motion of the spray to the entrainment and mixing region, after which it assists in autoignition of the spray mixture. Finally, exothermic reactions are induced in the spray mixture surrounding the autoignited spray.

Based on the results obtained with the LCR engine, when the spark timing is set to coincide with the maximum of the first heat release rate, the ignition timing of the second heat release is advanced, as shown in Fig. 8. During the trials involving combustion visualization in the constant volume vessel, however, a two-stage heat release rate process was not clearly observed. This apparent disparity may be due to variations in the temperature of the spray mixture. In the LCR engine, the gas temperature at the end of the

For Peer Review

compression stroke is approximately 550 K as the result of the pressure induced at the end of the stroke and the volumetric efficiency. In contrast, although the chamber pressure in the constant volume vessel is equal to the pressure at the end of the compression stroke of the LCR engine, the equilibrium calculation from gas composition and gas pressure indicates that the gas temperature is approximately 790 K. For this reason, heat release due to slow oxidation at lower temperatures was not observed in the constant volume vessel and so a two-stage heat release, such as is seen in Fig. 8, is not evident in Figs. 14 and 15.

It is worthwhile to inquire as to the reason why auto-ignition is induced by spark discharge. This phenomenon appears to result from a spark gap internal to the spray mixture, such that the mixture generates a kernel for autoignition on spark discharge and this kernel subsequently moves to an ignitable spray mixture formed from the spray flow or swirl flow. In the constant volume vessel, the swirl motion is negligible but spray flow is observed, whereas in the LCR engine there is a weak swirl but its effect is not negligible. In the future, we plan to carry out additional observations with the aim of confirming SICI combustion in a cylinder using an LCR engine.

For Peer Review

5. CONCLUSIONS

This study demonstrated a novel combustion system in which autoignition is induced by spark discharge into a pre-mixture formed during a long ignition delay time in a low compression ratio direct injection diesel engine. The results of this study can be summarized as follows:

(1) A combustion-mode diagram demonstrated that SICI combustion occurred at a relatively low load, an engine speed of 1800 rpm and a volumetric efficiency of 34 %, all of which approximate engine restart conditions.

(2) The highest advancement of autoignition timing induced by SICI combustion during these experimental trials was approximately 5° CA, suggesting that active control of autoignition timing by means of adjusting spark timing is possible.

(3) Based on visual observations of combustion, the advancement of autoignition timing is caused by the transportation of an ignition kernel generated by spark discharge.

ACKNOWLEDGMENTS

This work was financially supported by a Grant-in Aid for Scientific Research (C) (22560205) from The Ministry of Education, Culture, Sports, Science and Technology(MEXT) in Japan and by The Naoji Iwatani Foundation in 2012. The authors

For Peer Review

would like to thank Mr. Y. Takemura and Mr. K. Wakayama, undergraduate students from The University of Shiga Prefecture, for their assistance in the experimental trials. The authors would also like to thank the Lion Co. and the Diamond Electrics Co. for their donation of material and other forms of support.

For Peer Review

REFERENCES

[1] Koyama T., Fujiwara K., Nagae M., Ito T., Ohki H., Tomoda A., Study of the technology for low compression ratio in passenger car diesel engines", Trans. of JSAE Vol.42, No.3, pp.747-752, 2011 (In Japanese)

[2] Inagaki K., Mizuta J., Fuyuto T., Hashizume T., Ito H., Low emissions and high-efficiency diesel combustion using highly dispersed sprays with restricted in-cylinder swirl and squish flows -Proposal of combustion concept and validation of fundamental engine performance using single-cylinder engine-, Trans. of JSAE, Vol.42, No.1, 219-224, 2011 (In Japanese)

[3] Miyamoto N., Kamio M., Murayama T., Fukazawa S., A Study of low compression ratio diesel engines –2nd Report: Effect of combustion chamber configuration of DI diesel engines-", Trans. of JSME, Vol.38, No.307, 623-632, 1970 (In Japanese)

[4] Ward, M. A. V., Spark-ignited diesel engine, U. S. Army Tank-Automotive Command Research Development & Engineering Center, Technical Report, No.13502, Nov.1990, Approved for public release, 20031219023

[5] Dhinagar S., Nagalingam B., and Gopalakrishnan K., Spark Assisted Diesel Operation in a Low Compression Ratio Low Heat Rejection Engine," SAE Technical Paper 920545, 1992, doi:10.4271/920545

[6] Fritz S. and Abata D., A Photographic Study of Cold Start Characteristics of a Spark Assisted Diesel Engine Operating on Broad Cut Diesel Fuels, SAE Technical Paper 871674, 1987, doi:10.4271/871674

[7] Phatak R. and Komiyama K., Investigation of a Spark-Assisted Diesel Engine, SAE Technical Paper 830588, 1983, doi:10.4271/830588

[8] Persson H., Johansson B., Remón A., The Effect of Swirl on Spark Assisted Compression Ignition(SACI), SAE Technical Paper 2007-01-1856, 2007, doi:10.4271/2007-01-1856

[9] Ando H., Sakai Y., Fukano K., Shuu M., Kuwahara K., Possibility of ignition delay shortening by plasma-support, Trans. of JSAE, Vol.42, No.2, 397-402, 2011(In Japanese)

For Peer Review

[10] Kuwahara K., Sezaki T., Yamamoto Y., Shichi T., Furutani M., Ohta Y., Sakai Y., Ando H., Thermal ignition promotion by spark discharge synchronized with LTO, Trans.of JSAE Vol.42, No.1, 163-168, 2011(In Japanese)

[11] Nagamine Y., Shiina R., Kishimoto H., Araki M., Nakamura H., Shiga S., Kajitani S., Possibility of Applying HCCI Combustion to a 2-Stroke Engine Fueled with DME, 21st Symposium on Internal Combustion Engine of Japan, Okayama, 279-284, 2010(In Japanese)

[12] Kawasaki K., Ikawa T., Yamane K., Diesel Combustion and Emission Characteristics of FAME Having Same Ignition Quality as Gas Oil, Trans. of JSAE Vol.41, No.4, 865-870, 2010(In Japanese)

[13] Kondo C., Kumazawa N., Yamane K., Kawasaki K., Low Compression Ratio Diesel Engines by Means of FAME with High Cetane and High Volatility, Trans. of JSAE Vol.42, No.5, 1111-1116, 2011(In Japanese)

For Peer Review

Table and Figure captions

For Peer Review

Figure 11. Combustion modes associated with various values of the interval between spark and injection timing (θ_{sp} - θ_j) and injection timing

Figure 12. Improvement of engine re-starting

Figure 13. Variations in IMEP from the onset of fuel injection with and without spark discharge

Figure 14. Combustion without spark discharge

Figure 15. Combustion with spark discharge

Figure 16. Mechanism of ignition by SICI

For Peer Review

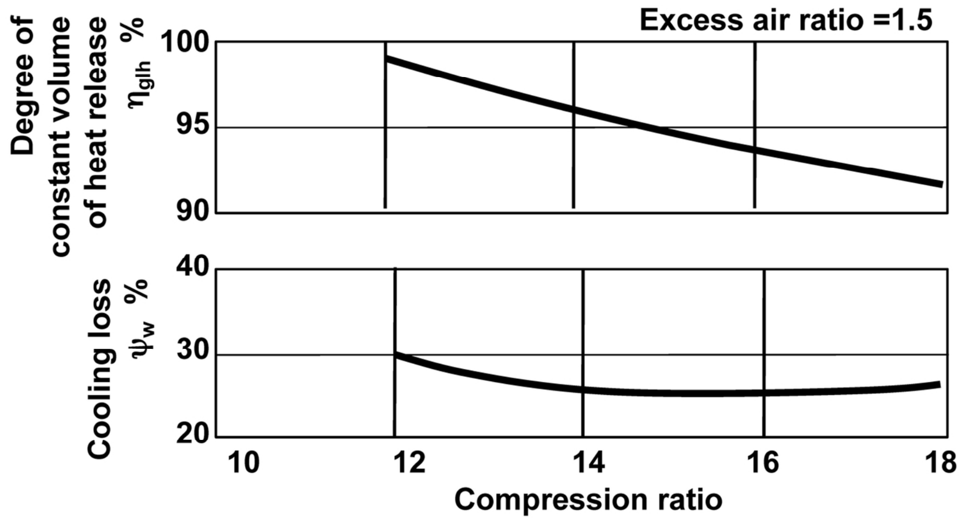

Figure 1 Effect of compression ratio on ψ_w and η_{glh}. From ref. [3]
125x68mm (300 x 300 DPI)

Peer Review

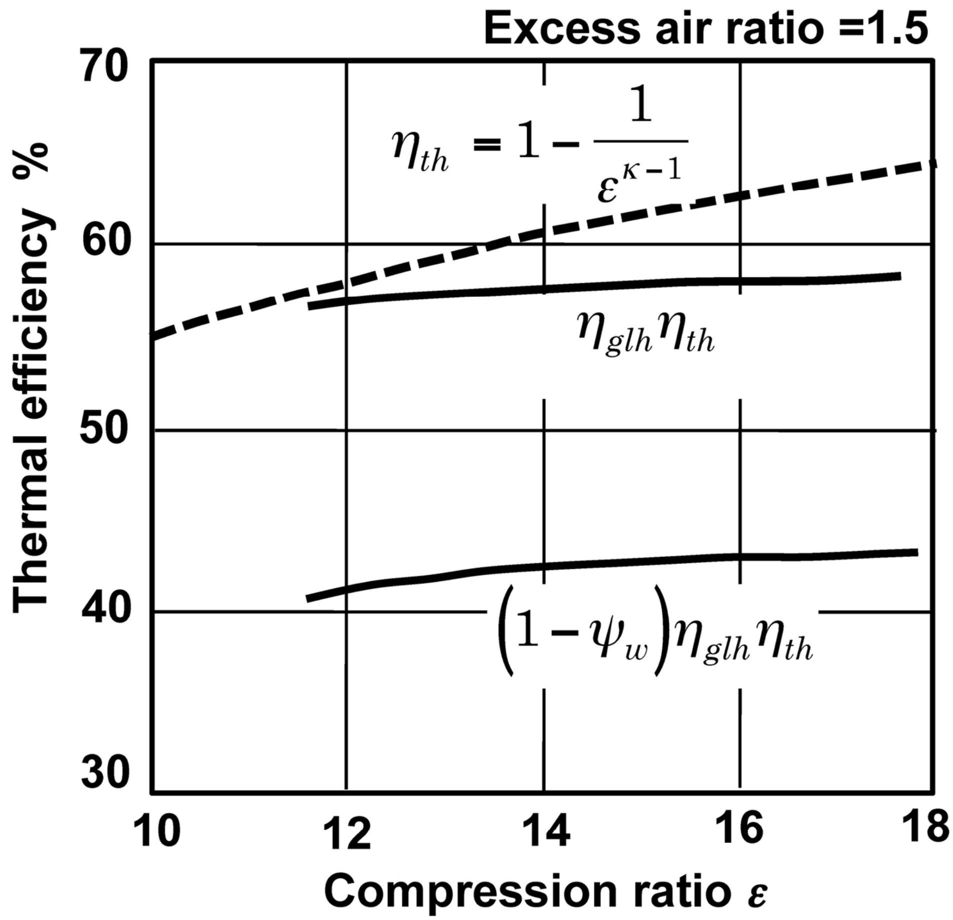

Figure 2. Variations in theoretical thermal efficiency based on expressions involving ψ_w and η_{glh}. From ref. [3]
146x139mm (300 x 300 DPI)

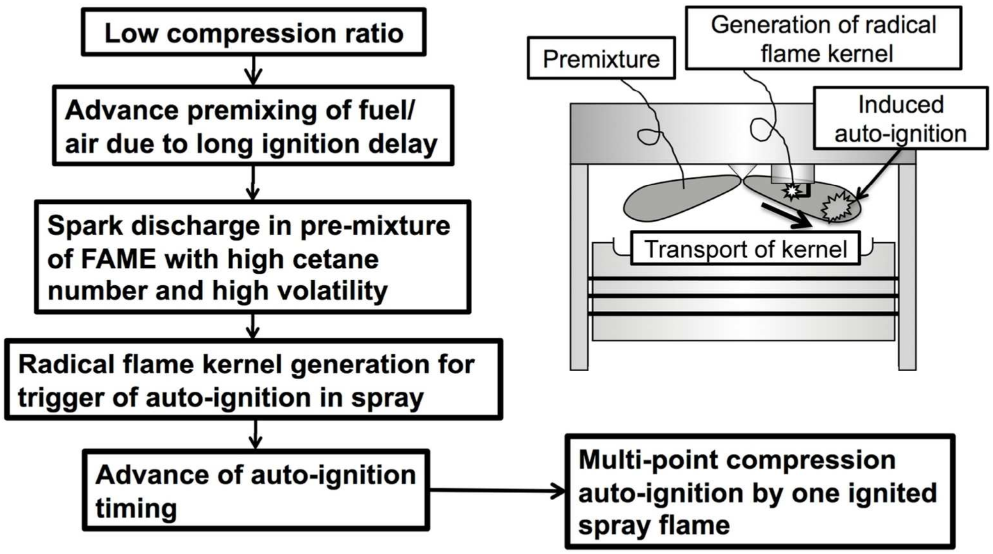

Figure 3 The SICI combustion system as proposed in this study
130x73mm (300 x 300 DPI)

er Review

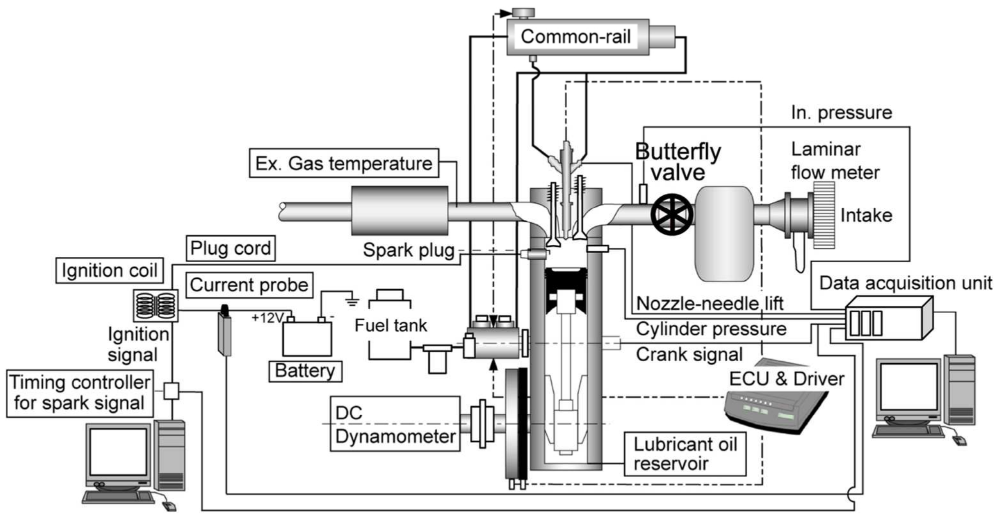

Figure 4 Schematic illustration of experimental set up
124x64mm (300 x 300 DPI)

Peer Review

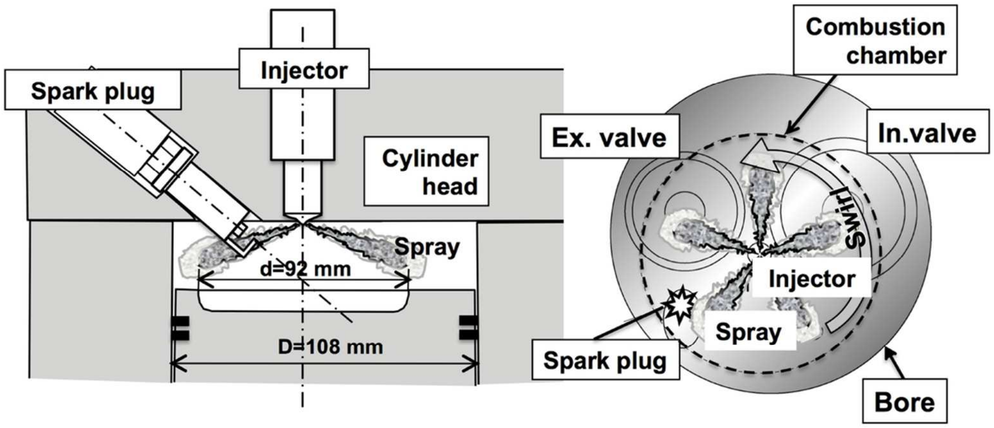

Figure 5 Positioning of the spark plug and injection nozzle
102x44mm (300 x 300 DPI)

Peer Review

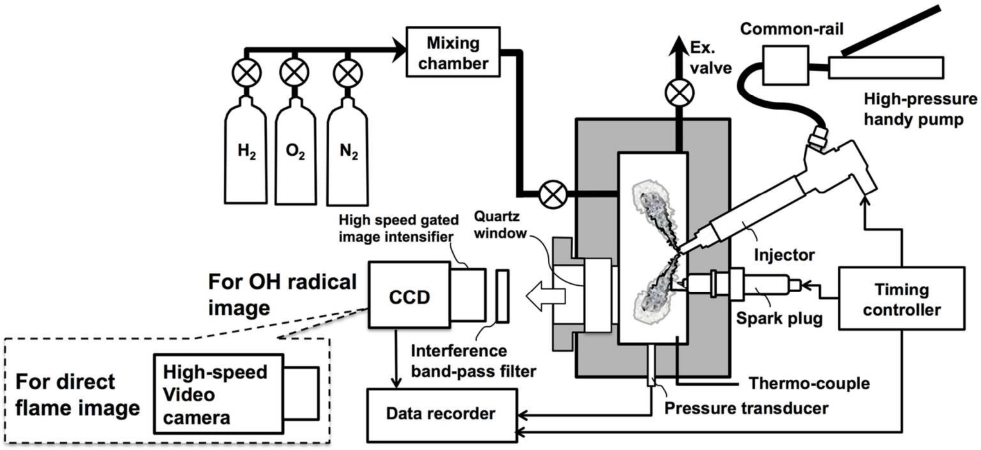

(a)

Figure 6(a)
144x71mm (300 x 300 DPI)

Peer Review

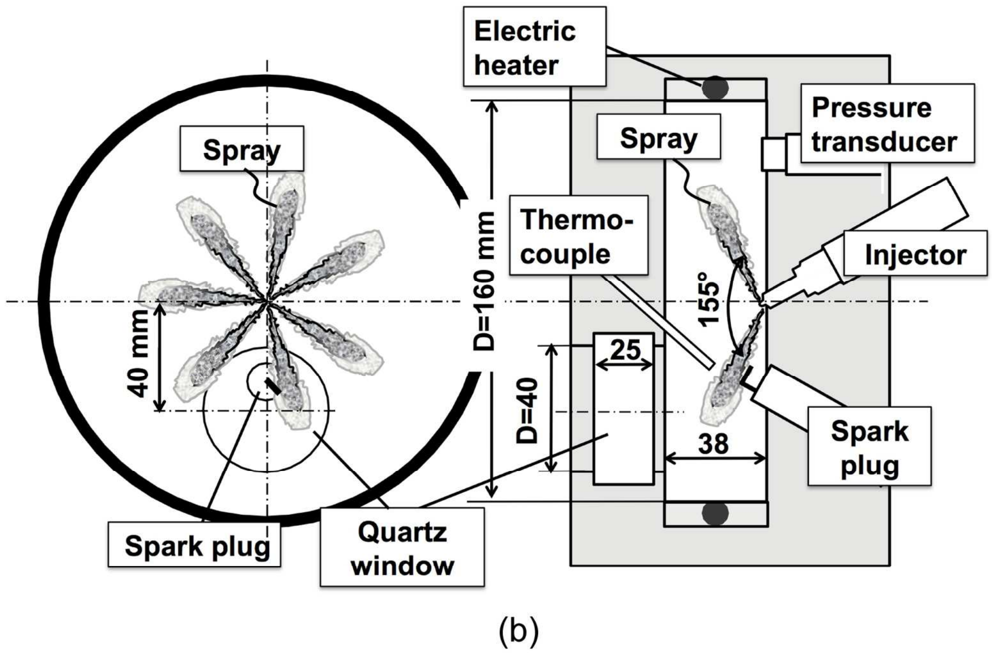

Figure 6(b) Experimental set up for visualization of ignition and combustion in a constant volume combustion vessel
165x110mm (300 x 300 DPI)

Review

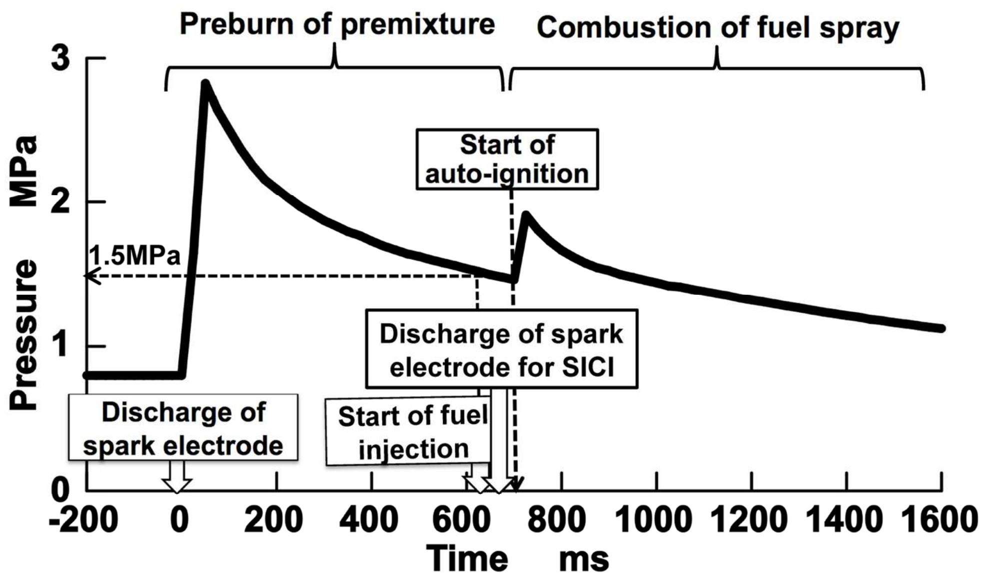

Figure 7 Pressure variations over time in a constant volume combustion vessel resulting from H2 preburning and autoignition by fuel injection
139x83mm (300 x 300 DPI)

For Peer Review

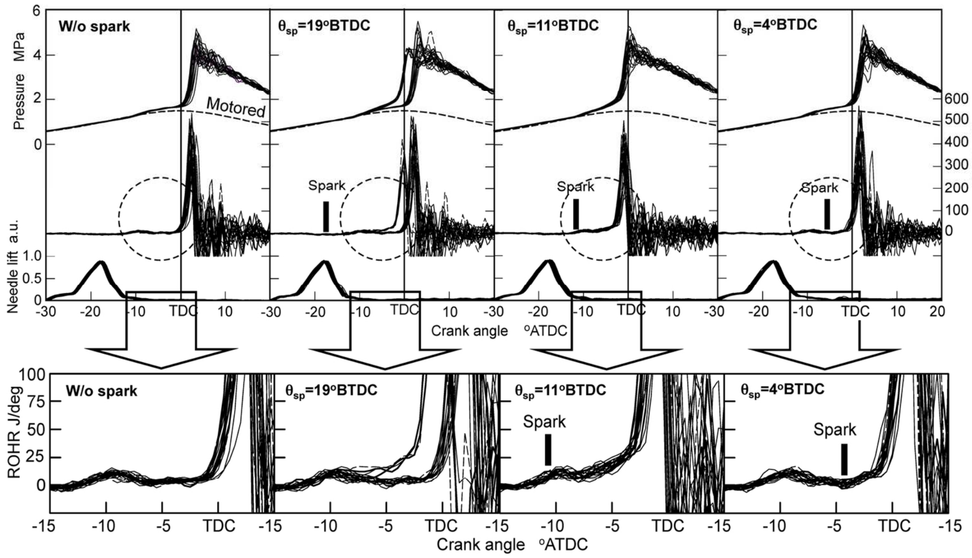

Figure 8 Variations in cylinder pressure, heat release rate and nozzle needle lift associated with three spark timing without spark discharge
150x87mm (300 x 300 DPI)

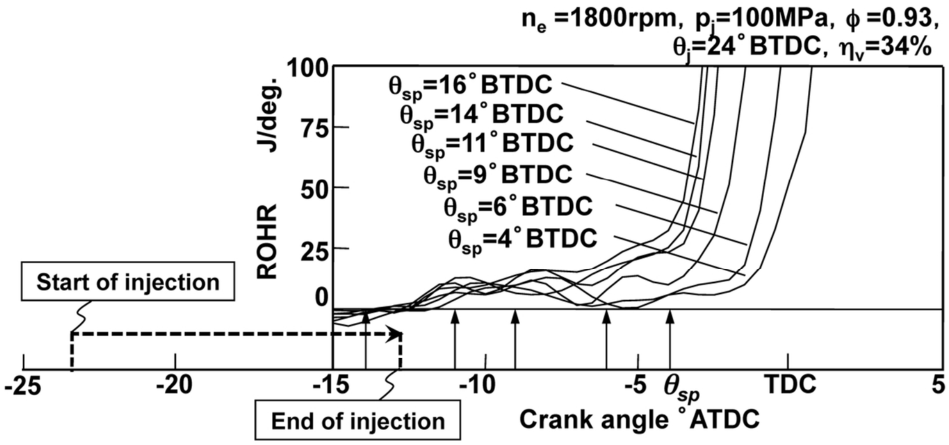

Figure 9 Effects of spark discharge timing on ignition timing and heat release rates
108x48mm (300 x 300 DPI)

Peer Review

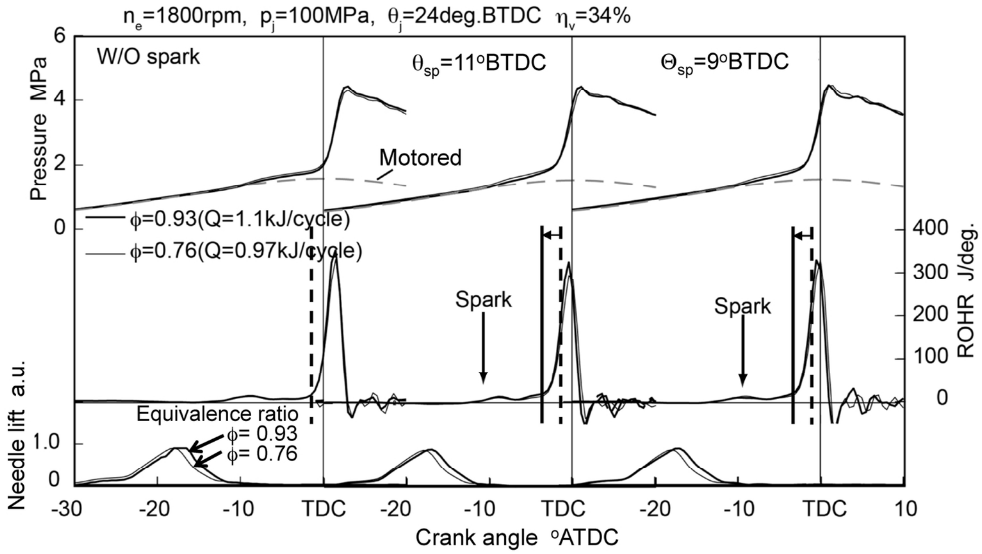

Figure 10 Effect of the equivalence ratio(φ) on SICI combustion
131x74mm (300 x 300 DPI)

Peer Review

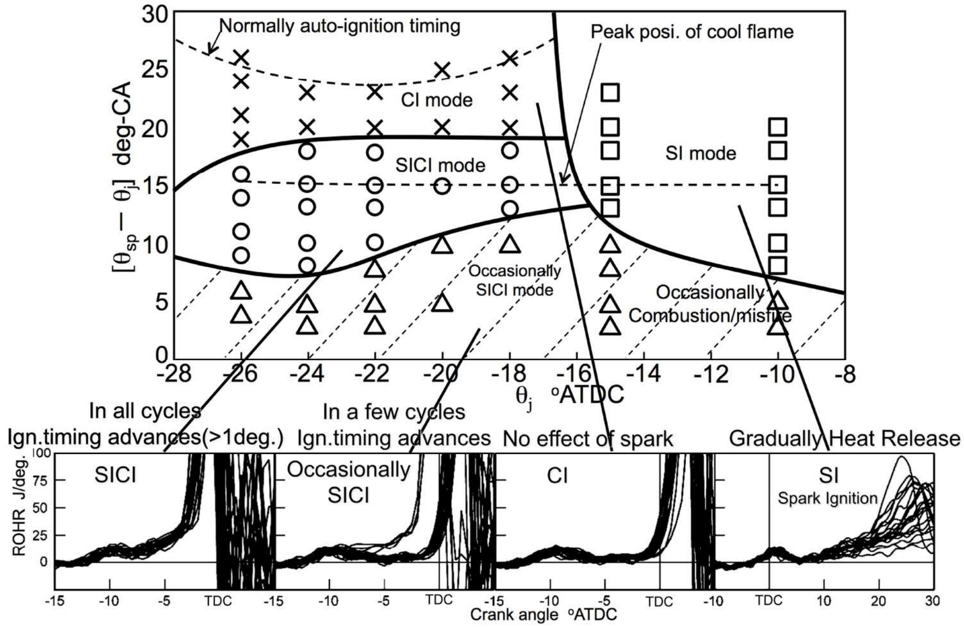

Figure 11 Combustion modes associated with various values of the interval between spark and injection timing (θ_{sp}-θ_j) and injection timing
168x110mm (300 x 300 DPI)

Review

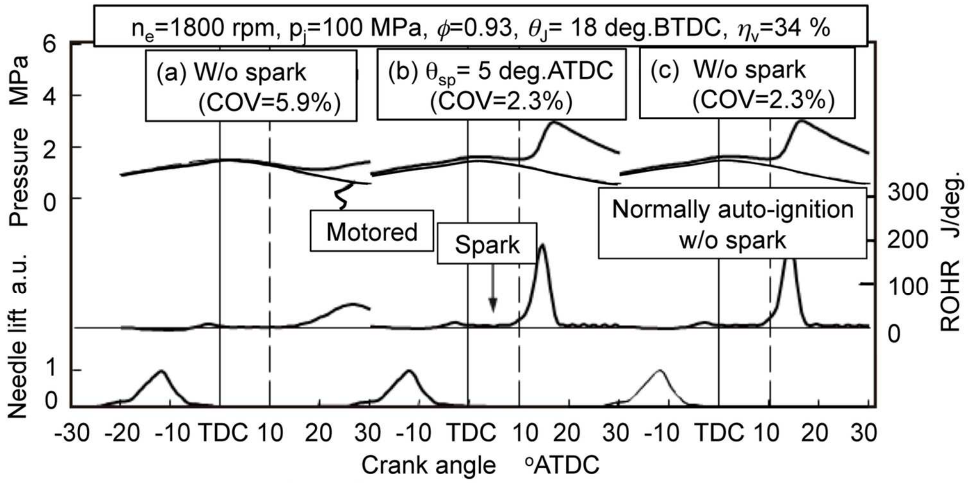

Figure 12 Improvement of engine re-starting
131x68mm (300 x 300 DPI)

Peer Review

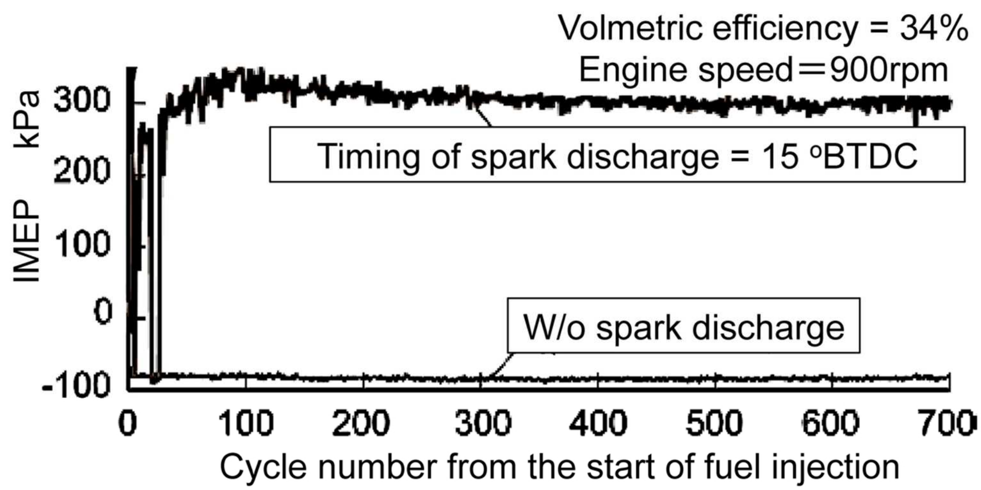

Figure 13 Variations in IMEP from the onset of fuel injection with and without spark discharge
111x56mm (300 x 300 DPI)

eer Review

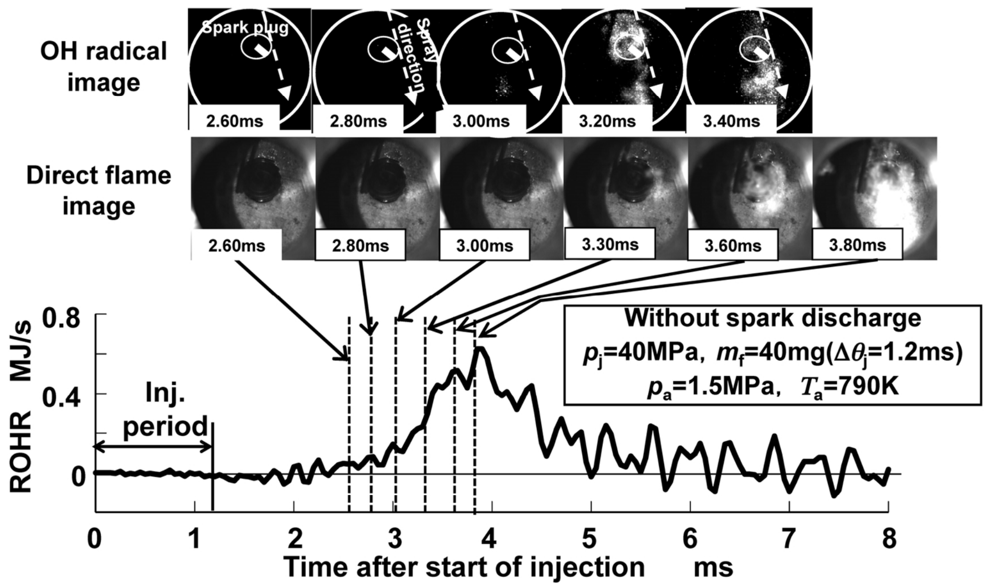

Figure 14 Combustion without spark discharge
148x88mm (300 x 300 DPI)

er Review

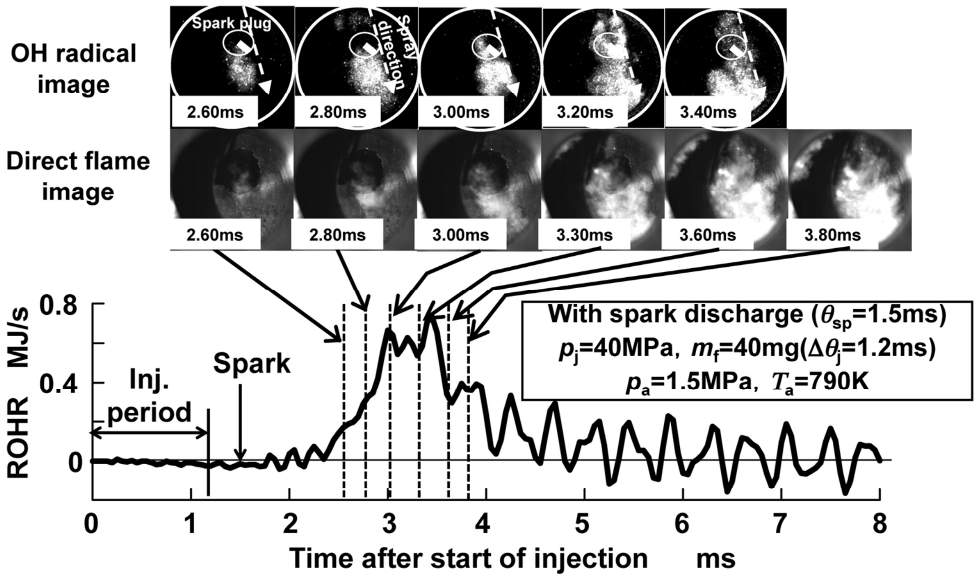

Figure 15 Combustion with spark discharge
148x88mm (300 x 300 DPI)

Peer Review

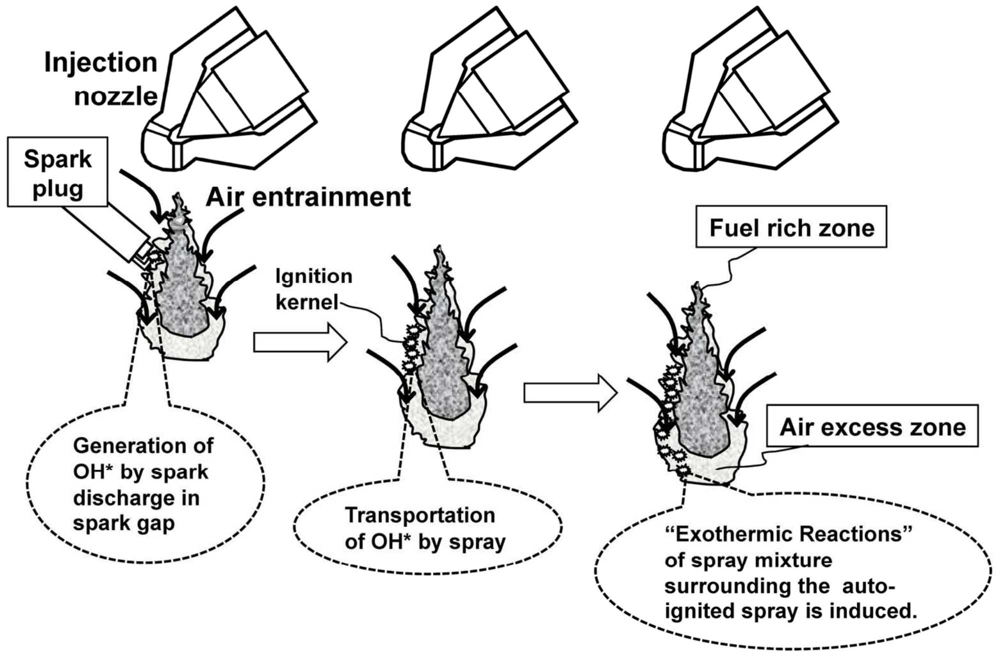

Figure 16 Mechanism of ignition by SICI
150x99mm (300 x 300 DPI)

Review

	LaME ($C_{13}H_{26}O_2$)	Diesel (JIS No.2)
CN_{CFR}	61.4	56
Distillation T10 ℃	-	215
T50 ℃	-	272
T90 ℃	-	338
Boiling point ℃	266	-
LHV MJ/kg	35.2	42.7
Oxygen wt%	15.0	<0.1

Table 1 Primary specifications of the experimental fuel
139x84mm (300 x 300 DPI)

er Review

	FD-1（Nissan Diesel）
Type	Direct Injection，Single cylinder, Natural aspirated, Water-cooled
Displacement	1053cm^3
Compression ratio	14 (Original: 18.1)
Piston shape	Shallow dish with flat bottom (Original: Toroidal)
Fuel injection system	Common-rail injection system (Denso ECD-U2)
Injection nozzle	5 holes-0.18mm
Swirl ratio	0.7

Table 2 Primary specifications of the experimental test engine
156x109mm (300 x 300 DPI)

Review